

THE DETERMINATION OF PHOTON DETECTION EFFICIENCY  
PARAMETERS FOR LITHIUM-DRIFT GERMANIUM DETECTORS

by \

Gary Paul Agin

B. S., University of Kansas, 1963

---

A MASTER'S THESIS

submitted in partial fulfillment of the

requirements for the degree

MASTER OF SCIENCE

Department of Physics

KANSAS STATE UNIVERSITY  
Manhattan, Kansas

1967

Approved by:

C. E. Manderville  
Major Professor

## TABLE OF CONTENTS

INTRODUCTION . . . . .	1
GAMMA RAY INTERACTIONS WITH MATTER . . . . .	3
DETERMINATION OF DETECTOR PARAMETERS . . . . .	7
DETERMINATION OF RELATIVE INTENSITIES . . . . .	40
APPENDIX . . . . .	51
ACKNOWLEDGMENT . . . . .	57
BIBLIOGRAPHY . . . . .	58

## INTRODUCTION

The measurement of the relative intensities of the gamma rays emitted in the decay of a radioactive isotope is useful in determining certain properties of the nuclear energy states. When used with beta-gamma coincidence data, gamma-gamma coincidence data, and measured internal conversion coefficients the spins and parities of the nuclear states may be determined.

The first step in determining the relative intensities of the gamma rays is the detection of the radiation and the accumulation of differential pulse height spectra. In the present work two lithium drifted germanium PIN diodes, Ge(Li) detectors, were used. The theory of operation of these detectors has been explained previously (6,7,12). The pulse height spectra were accumulated in commercial multichannel analyzers using analog to digital conversion and random access digital memories (12).

Several problems prevent one from determining relative intensities by simple observation of the spectrum in the analyzer. Since one is interested in the intensities of the gamma rays emitted from a radioactive source, the effects of any intervening absorbers must be taken into account. The probability of a gamma ray interacting with the detector is not constant with energy. Thus this variation in detector efficiency introduces another correction. Finally, the probability of a gamma ray interacting by any one mode of interaction over another is not constant and another correction results. All of the above probabilities (cross-sections) are tabulated (13) and

their effects may be calculated from theory. However, no table of probabilities is available for the chance of a gamma ray interacting two or more times with the detector and eventually depositing all of its energy in the detector. This effect depends upon detector size and geometry. Thus at least one experimental measurement is necessary to determine the response of the detector.

The measurement of the full energy peak to total ratio, and the calculation of the detection efficiency are described. Using these parameters, the relative intensities of gamma rays in the radioactive decay of  $\text{Mo}^{99}$  and  $\text{Br}^{82}$  are found.

## GAMMA RAY INTERACTIONS WITH MATTER

There are a number of processes by which gamma rays interact with matter. An understanding of these is necessary to interpret the response of the detector. Since it is necessary that the gamma rays deposit energy in the Ge(Li) crystal for their presence to be detected, the interaction processes which remove energy from the gamma rays are the ones of interest. These are the Compton effect, the photoelectric effect, and pair production. Each of these are discussed and the other processes are mentioned.

### Compton Effect

In the Compton effect incident gamma rays undergo elastic collisions with free electrons. An electron in the Ge crystal may be considered free if the gamma ray energy is greater than the binding energy of Ge, 11.103 keV. The application of the laws of conservation of energy and momentum to this process leads to the expression

$$E'_\gamma = \frac{E_\gamma}{1 + \frac{E_\gamma}{m_0 c^2} (1 - \cos \Theta)}$$

where  $E_\gamma$  is the energy of the incident gamma ray,  $E'_\gamma$  is the energy of the recoil gamma ray,  $m_0$  is the rest mass of the electron,  $c$  is the speed of light, and  $\Theta$  is the angle at which the recoil gamma ray is scattered (5).

The kinetic energy of the recoil electron may easily be found to be

$$E_e = \frac{E_\gamma}{1 + m_0 c^2 / E_\gamma (1 - \cos \Theta)}$$

From these relations one can see that the recoil electron energy spectrum will extend from zero energy, for  $\Theta = 0^\circ$ , to a maximum energy, for  $\Theta = 180^\circ$ , which is given by

$$E_{e_{\max}} = E_C = \frac{E_\gamma}{1 + \frac{m_0 c^2}{2 E_\gamma}}$$

where  $E_C$  is called the Compton edge energy. The Compton interaction is the dominant mode by which gamma rays interact with Ge in the energy interval from 200 keV to 8 MeV (6).

#### Photoelectric Effect

In the photoelectric effect all of the energy of the incident gamma ray is absorbed by a bound electron of a Ge atom, appearing as kinetic energy of this electron as it is ejected from the atom. The kinetic energy of this ejected electron will be equal to the difference between the incident gamma ray energy and the binding energy of the atomic shell from which the electron was ejected. The remainder of the energy appears as characteristic X-rays and Auger electrons emitted by the filling of the vacancy in the atomic shell (5). The photoelectric effect is the primary mode of interaction in Ge for gamma rays of energies below 200 keV.

Usually all of the X-rays and electrons are detected by the Ge(Li) detector and the spectrum due to the photoelectric effect appears as a single peak. Sometimes, however, the X-rays may escape, yielding a secondary peak at an energy of  $E_\gamma - E_x$  where  $E_\gamma$  is the energy of the incident gamma ray and  $E_x$  is the X-ray energy.

## Pair Production

At gamma ray energies above 1.02 MeV, the process of pair production becomes increasingly important. In this interaction the gamma ray is completely absorbed and in its place appears a positron-electron pair whose total energy, including rest mass energy, is equal to the gamma ray energy. This process occurs only in the field of charged particles since they are necessary for the conservation of momentum (5).

This effect is most easily explained in terms of the Dirac electron theory, which considers positrons as holes in an otherwise filled sea of negative energy states of electrons. When the incident gamma ray interacts, it is thought to raise one of the electrons with negative energy to a state of positive energy, requiring a gamma ray energy of  $2m_0c^2$ . Thus both a positron and an electron are created at the same time with the excess gamma ray energy going into kinetic energy of the pair (5).

## Other Effects

There are six other processes by which gamma rays may interact with matter, all of which are negligible. Each is discussed briefly (5).

In Rayleigh scattering the incident gamma ray is scattered elastically by the atomic electrons. This effect is neglected here because it does not deposit energy in the detector.

In Thomson scattering the incident gamma ray is scattered elastically by the nucleus. The effect is small due to the large mass of the nucleus

and again is neglected since it does not deposit energy in the detector.

Delbruck scattering has been proposed but not observed experimentally. In this process the incident gamma rays scatter elastically with the electric field surrounding the nucleus.

In nuclear resonance scattering the gamma rays scatter inelastically with the nucleus exciting a nuclear level with reemission of the energy. This effect is not normally observed.

The incident gamma ray may be completely absorbed by the nucleons followed by the disintegration of the nucleus. This occurs only when the gamma ray energy is greater than the separation energy for a nucleon and is confined to a region above 8 MeV. The probability of this occurring is negligible when compared to the Compton effect and pair production.

Finally, the gamma ray may produce mesons. This effect occurs only for a gamma ray energy greater than 150 MeV and its probability is negligible.



## DETERMINATION OF DETECTOR PARAMETERS

The experimental measurement of the full energy peak to total ratio and the calculation of the detector efficiency were necessary for the determination of relative gamma ray intensities. Two Ge(Li) detectors were used. One, manufactured by RCA Victor of Canada, Ltd., had a sensitive thickness of 2 mm and was 18.5 mm in diameter. The other, manufactured by Solid State Radiations, Inc. (SSR), had a sensitive thickness of 4.2 mm and an area of 100 mm<sup>2</sup>.

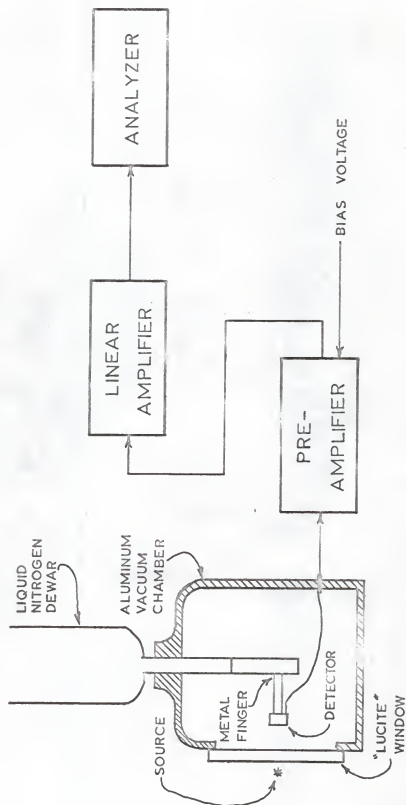
## Full Energy Peak to Total Ratio

The full energy peak to total ratio was determined using the detector-source geometry used by the Nuclear Physics group at Kansas State University to study radioactive isotopes. The Ge(Li) detector was mounted in an aluminum vacuum chamber on a metal finger in contact with liquid nitrogen. The vacuum chamber was necessary to prevent water vapor in the atmosphere from condensing on the surface of the detector. On one side of the vacuum chamber, facing the front of the detector, was a 1/4-inch thick clear "Lucite" window. This window allowed one to position the source on the centerline of the detector visually. It was of a lower Z than the aluminum sides of the vacuum chamber and thus transmitted low energy gamma rays more readily. The source of radiation was placed directly upon the "Lucite" window in order to obtain the largest possible solid angle and thus the highest counting efficiency. Plate I shows the geometry used and a block diagram of the

# EXPLANATION OF PLATE I

A schematic drawing of the physical geometry used to accumulate data and a block diagram of the electronics.

## PLATE I



electronics.

The signals from the Ge(Li) detector were first amplified in a charge sensitive preamplifier, Tennelec Model 100C, with a charge sensitivity of  $0.21 \mu\text{v}$  per ion pair and an integral nonlinearity of 0.3% of maximum output as given in the manufacturer specifications. From the preamplifier, the signal went through a linear amplifier, Tennelec Model TC 200. This amplifier had RC pulse shaping and a total amplifier gain of 4 to 2048, adjustable, with an integral nonlinearity of less than 0.05% of rated output as given by the manufacturer specifications.

Two analyzers were used in the accumulation of the data. A Technical Measurement Corporation Model 404-6 400-channel Pulse Height Analyzer was used in the determination of the ratio for the RCA Ge(Li) detector. The data were recorded on punched paper tape. A Technical Measurement Corporation 4096-channel Multiparameter Pulse Analyzer System with Model 213 Pulse Height Logic Units was used in the determination of the ratio for the SSR Ge(Li) detector. This unit had an integral linearity of  $\pm 0.5\%$  of full scale. The 4096 system was used in the singles mode with an analog to digital converter range of 512 channels. The data were recorded on magnetic tape.

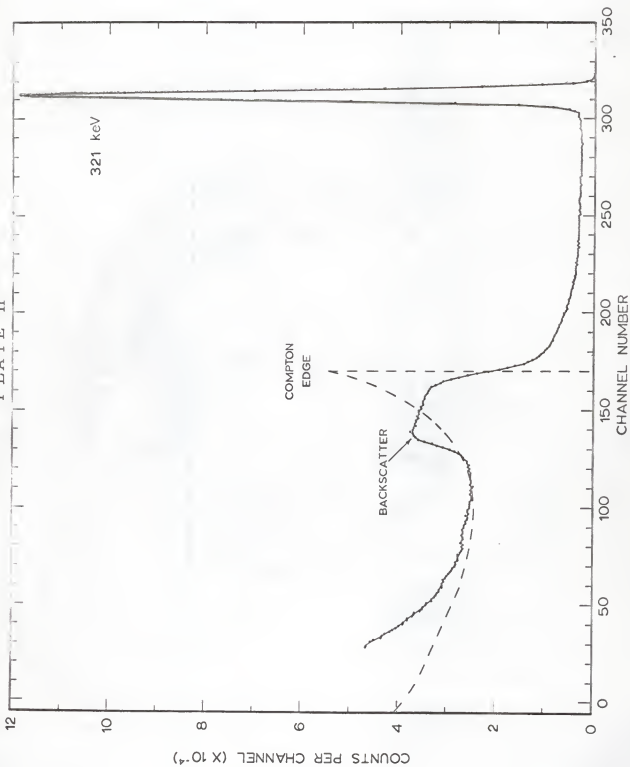
The spectra shown in Plates II-V were accumulated with the RCA Ge(Li) detector. Those shown in Plates VI-X were accumulated with the SSR Ge(Li) detector.

Internal energy calibration points were used to determine the position of energy zero. It was found that bremsstrahlung radiation from the

## EXPLANATION OF PLATE II

$\text{Cr}^{51}$  gamma ray spectrum accumulated with the RCA 2 mm thick Ge(Li) detector. The dashed line is the theoretical Compton distribution used in the calculation. The peak to total ratio for the 321 keV gamma ray is 0.113.

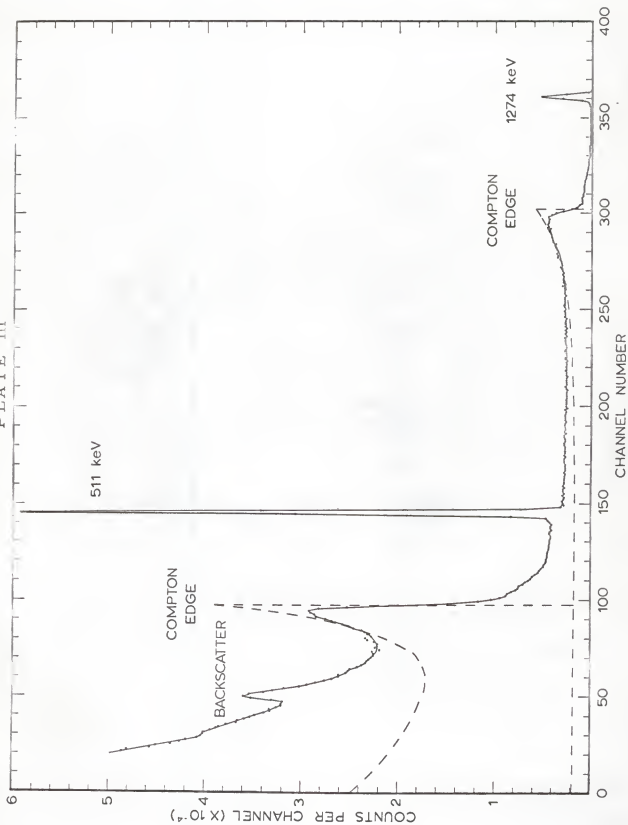
PLATE II



### EXPLANATION OF PLATE III

$\text{Na}^{22}$  gamma ray spectrum accumulated with the RCA 2 mm thick Ge(Li) detector. The dashed lines are the theoretical Compton distributions used in the calculations. The peak to total ratio for the 511 keV gamma ray is 0.065. The peak to total ratio for the 1274 keV gamma ray is 0.019.

## PLATE III

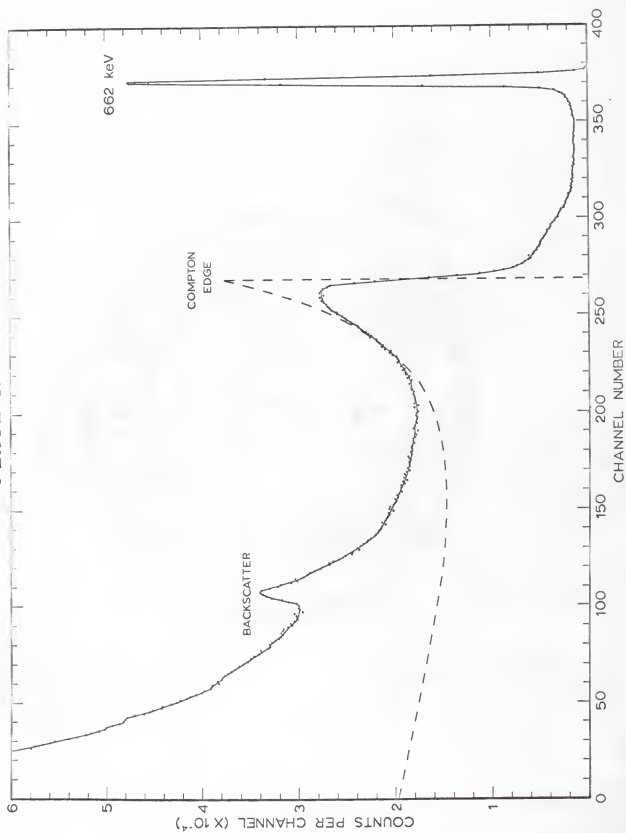




#### EXPLANATION OF PLATE IV

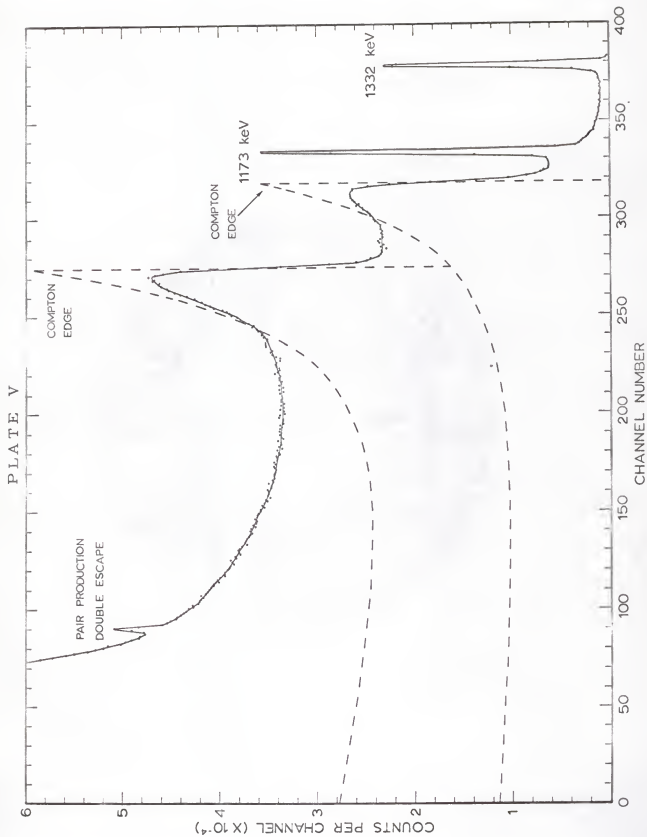
Cs<sup>137</sup> gamma ray spectrum accumulated with the RCA 2 mm thick Ge(Li) detector. The dashed line is the theoretical Compton distribution used in the calculation. The peak to total ratio for the 662 keV gamma ray is 0.038.

PLATE IV



#### EXPLANATION OF PLATE V

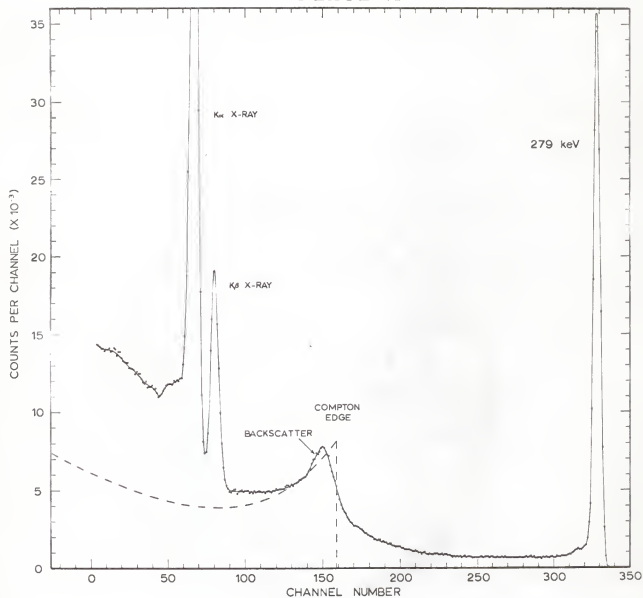
$^{60}\text{Co}$  gamma ray spectrum accumulated with the RCA 2 mm thick Ge(Li) detector. The dashed lines are the theoretical Compton distributions used in the calculations. The peak to total ratio for the 1173 keV gamma ray is 0.019. The peak to total ratio for the 1332 keV gamma ray is 0.016.



#### EXPLANATION OF PLATE VI

Hg<sup>203</sup> gamma ray spectrum accumulated with the SSR 4.2 mm thick Ge(Li) detector. The dashed line is the theoretical Compton distribution used in the calculation. The peak to total ratio for the 279 keV gamma ray is 0.205.

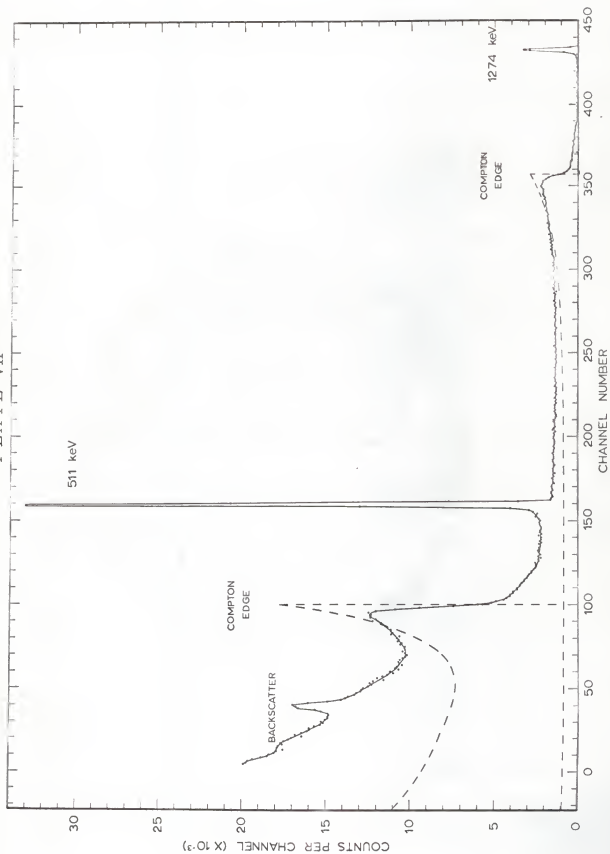
## PLATE VI



#### EXPLANATION OF PLATE VII

$\text{Na}^{22}$  gamma ray spectrum accumulated with the SSR 4.2 mm thick Ge(Li) detector. The dashed lines are the theoretical Compton distributions used in the calculations. The peak to total ratio for the 511 keV gamma ray is 0.064. The peak to total ratio for the 1274 keV gamma ray is 0.021.

## PLATE VII

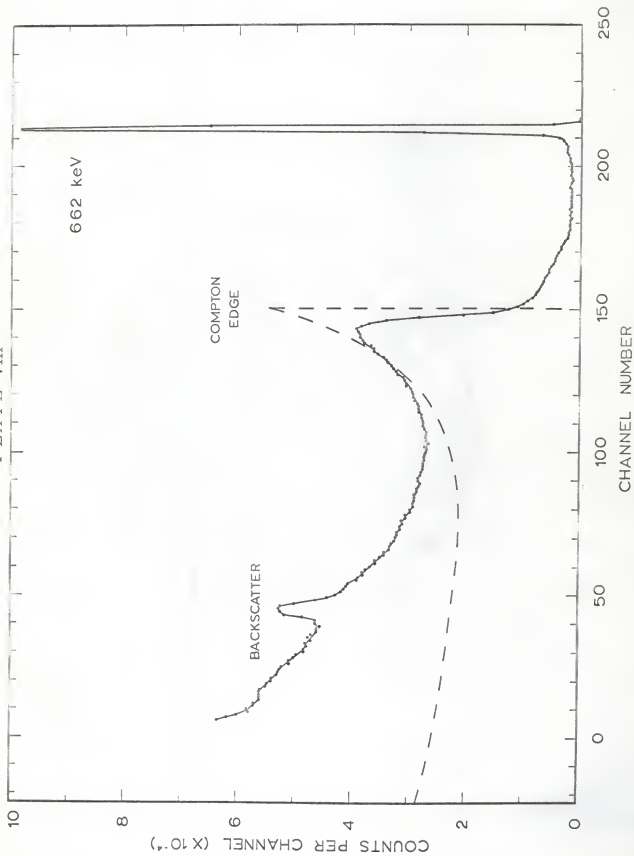




### EXPLANATION OF PLATE VIII

$\text{Cs}^{137}$  gamma ray spectrum accumulated with the SSR 4.2 mm thick Ge(Li) detector. The dashed line is the theoretical Compton distribution used in the calculation. The peak to total ratio for the 662 keV gamma ray is 0.044.

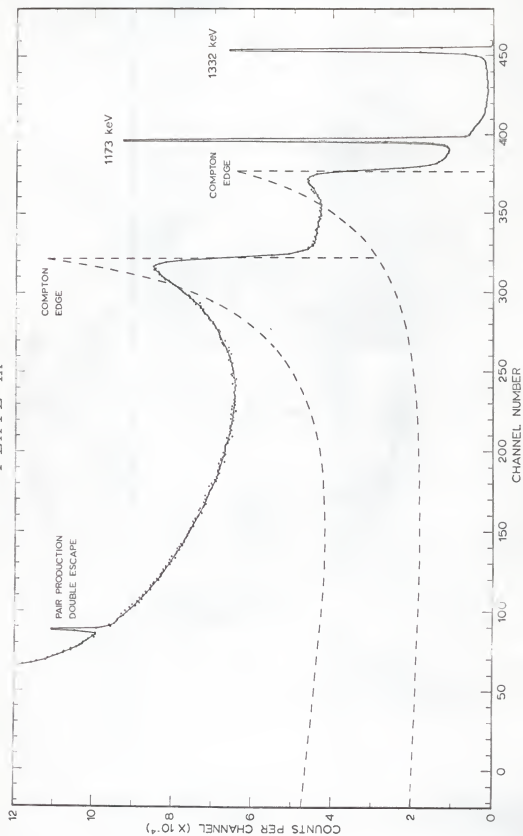
## PLATE VIII



### EXPLANATION OF PLATE IX

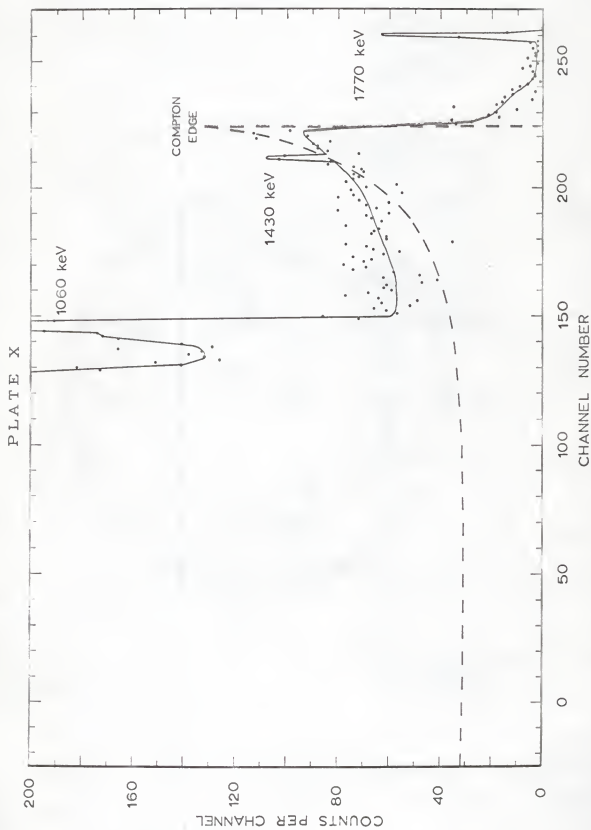
$\text{Co}^{60}$  gamma ray spectrum accumulated with the SSR 4.2 mm thick Ge(Li) detector. The dashed lines are the theoretical Compton distributions used in the calculations. The peak to total ratio for the 1173 keV gamma ray is 0.020. The peak to total ratio for the 1332 keV gamma ray is 0.017.

## P L A T E IX



### EXPLANATION OF PLATE X

Bi<sup>207</sup> gamma ray spectrum accumulated with the SSR 4.2 mm thick Ge(Li) detector. The dashed line is the theoretical Compton distribution used in the calculation. The low energy portion of the spectrum is not shown. The peak to total ratio for the 1770 keV gamma ray is 0.011.



beta decay of some of the sources, low energy gamma rays, or electronic noise prevented one from simply using the observed spectra to find the total number of counts due to a single gamma ray energy. A table of cross-sections giving the number of Compton electrons per unit energy for certain energy gamma rays was used (10). The cross-sections for the gamma ray energies used were found from this table by log-log interpolation and are given in Table 1. The cross-sections for each gamma ray energy were normalized to the observed spectrum by using an appropriate point near the Compton edge. This point was chosen to minimize the effects appearing at lower energies. This normalization was accomplished by determining the appropriate multiplicative factor necessary to make the chosen point coincide with the experimental curve. The other cross-sections were multiplied by this same factor to obtain the theoretical distribution. This theoretical distribution is indicated in Plates II-X as a dashed line.

The point chosen for normalization on Plate II,  $\text{Cr}^{51}$ , was at  $E/E_{\text{max}} = 0.7$  (126 keV). This point was used to avoid the effect of the back-scatter peak at 138 keV and electronic noise at lower energies. The normalization factor was found to be  $1.615 \times 10^{28}$ . The determination of the theoretical distribution for Plate II is shown in Table 2. A similar process yielded the distributions in Plates III-X.

The total number of counts was found by taking the area under the dashed line from energy zero up to the energy at which the theoretical and actual distributions matched and the area under the experimental curve from there to the gamma ray energy. The number of counts in the full energy

Table 1. Differential cross-section for the energy distribution of Compton electrons. The table gives the number of Compton electrons per MeV interval at energy E, per electron of material per photon per cm<sup>2</sup>. Multiply by 10<sup>-27</sup> to obtain  $d\sigma(E)/d\epsilon$  in cm<sup>2</sup> per electron (10).

E/E <sub>max</sub>	279	321	511	662	Gamma Ray Energy (keV)			1332	1770
	145	180	341	480	E <sub>max</sub>			1116	1548
0	3240	2517	980	585	190	159	145	145	80.5
.1	2940	2294	935	552	188	155	141	141	79.0
.2	2650	2080	850	520	177	150	136	136	78.0
.3	2480	1880	790	490	173	146	134	134	77.0
.4	2160	1707	738	465	166	143	130	130	77.0
.5	1970	1577	698	445	166	143	131	131	79.0
.55	----	----	680	436	167	145	133	133	81.0
.60	1920	1516	670	435	168	146	134	134	82.5
.65	----	----	685	444	173	150	138	138	86
.70	1980	1569	700	458	182	158	146	146	91
.75	----	----	730	482	195	170	157	157	99
.80	2270	1803	800	530	214	186	173	173	111
.85	----	----	900	594	246	215	200	200	129
.90	2950	2338	1050	705	292	259	241	241	158
.95	----	----	1290	870	382	339	314	314	213
1.00	4200	3385	1630	1130	580	490	458	458	330



Table 2. Theoretical Compton distribution in the  $\text{Cr}^{51}$  spectrum.

$E/E_{\text{max}}$	E (keV)	Channel Number	Cross- section $\times 10^{-27}$	Theoretical Counts	Experimental Counts
0	0	-6	2517	40500	---
.1	18	5	2294	37000	---
.2	36	24	2080	33600	82642
.3	54	42	1880	30400	38068
.4	72	60	1707	27500	31014
.5	90	79	1577	25400	26804
.6	108	97	1516	24400	25687
.7	126	115	1569	25300	25300
.8	144	134	1803	29100	33117
.9	162	152	2338	37800	35628
1.0	180	170	3385	54600	21879

peak was found by taking the area under the peak.

Plate XI shows a plot of peak to total ratio verses energy for the RCA Ge(Li) detector and Plates XII-XIII show the same for the SSR Ge(Li) detector. The errors shown for the points indicate only the statistical error in the data. No systematic errors are indicated. The dashed line on these plates indicates the ratio of the photoelectric cross-section to the total cross-section, the theoretical peak to total ratio.

The experimental curve falls above the theoretical curve due to multiple interactions in which all of the Compton scattered radiation is absorbed by the detector. The two curves would coincide if the detector was infinitesimal in size so that all of the scattered radiation would escape.

### Detector Efficiency

The definition of detection efficiency used was the ratio of the number of gamma rays detected to the number of gamma rays that entered the detector. This was sufficient since one was interested in the intensities of the gamma rays relative to each other and not their absolute intensities.

The detector was a cylinder with radius " $r$ ", thickness " $t$ " and total attenuation coefficient " $\mu(E)$ "; the point source was a distance " $h$ " away

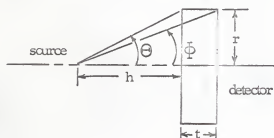


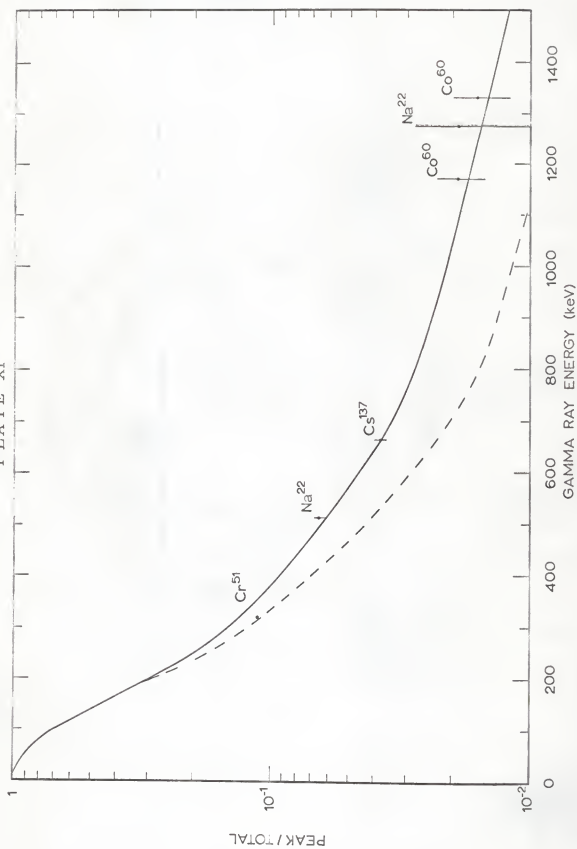
Fig. 1

from the face of the detector on the symmetry axis, see Fig. 1. With  $\Theta = \tan^{-1}(r/h)$  and  $\bar{\Phi} = \tan^{-1}(r/h+t)$ , the efficiency " $\epsilon(E)$ " at an energy " $E$ " was (14)

## EXPLANATION OF PLATE XI

A plot of the full energy peak to total ratio verses the gamma ray energy for the RCA 2 mm thick Ge(Li) detector. The dashed line is the ratio of the photo-electric cross-section to the total cross-section.

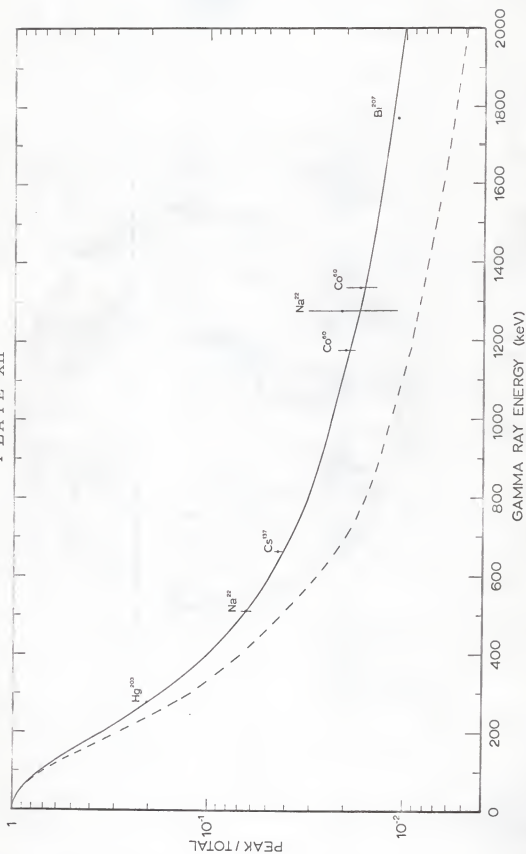
PLATE XI



## EXPLANATION OF PLATE XII

A plot of the full energy peak to total ratio verses gamma ray energy for the SSR 4.2 mm thick Ge(Li) detector. The dashed line is the ratio of the photoelectric cross-section to the total cross-section.

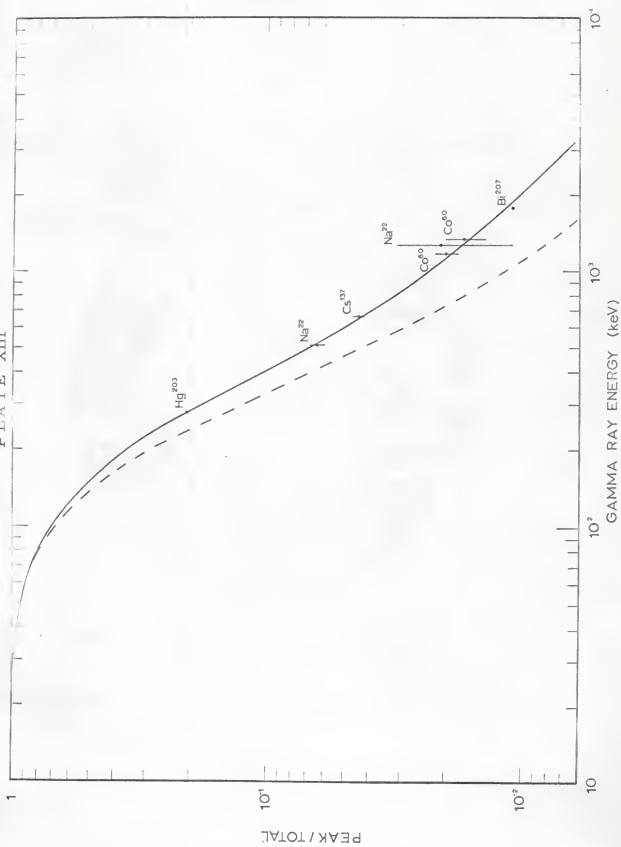
PLATE XII



### EXPLANATION OF PLATE XIII

A log-log plot of the full energy peak to total ratio verses gamma ray energy for the SSR 4.2 mm thick Ge(Li) detector. The dashed line is the ratio of the photoelectric cross-section to the total cross-section.

PLATE XIII





$$e'(E) = \frac{1}{1 - \cos \Theta} \left\{ \int_0^{\frac{\pi}{2}} \left[ 1 - e^{-\frac{\mu(E)t}{\cos \Theta}} \right] \sin \Theta \, d\Theta \right. \\ \left. + \int_{\frac{\pi}{2}}^{\Theta} \left[ 1 - e^{-\mu(E) \left( \frac{r}{\sin \Theta} - \frac{h}{\cos \Theta} \right)} \right] \sin \Theta \, d\Theta \right\}$$

Since a correction for the effect of intervening absorbers was necessary, it was decided to include this correction in the efficiency calculation. Thus the efficiency was

$$e(E) = e'(E) \exp(-\sum_i \mu_i(E) t_i)$$

where each  $\mu_i$  and  $t_i$  were the total attenuation coefficient and thickness of each absorber (13).

A FORTRAN computer program was written to calculate these efficiencies. A listing of the complete program appears in the Appendix. This program was run on Kansas State University's IBM 1401-1410 computer and the results used in the following calculation of relative intensities.

## DETERMINATION OF RELATIVE INTENSITIES

The relative intensities of the gamma rays of two radioactive isotopes were found. When compared to previous intensity determinations there is close agreement. Additional merit of Ge(Li) detectors over NaI(Tl) is better energy resolution and consequently better intensity determination.

After the detector parameters were determined, the area under each gamma ray peak was found. These quantities were the "raw data." The raw data was divided by the detection efficiency and the peak to total ratio to find the corrected data. This was the actual number of gamma rays entering the detector. The corrected data was normalized to one gamma ray whose intensity was called 100.

The spectra obtained from the beta decay of  $\text{Mo}^{99}$  are shown in Plates XIV-XV. The relative intensities calculated from these data are shown in Table 3. Also included in this table are the relative intensities quoted in previous work.

The spectra obtained from the beta decay of  $\text{Br}^{82}$  are shown in Plates XVI-XVII. The relative intensities calculated from these data are shown in Table 4. This table also included the relative intensities quoted in previous work.

#### EXPLANATION OF PLATE XIV

The low energy gamma ray spectrum of  $\text{Mo}^{99}$  accumulated with the SSR 4 mm thick Ge(Li) detector. No absorbers were used between the source and the detector.



#### EXPLANATION OF PLATE XV

The high energy gamma ray spectrum of  $\text{Mo}^{99}$  accumulated with the SSR 4 mm thick Ge(Li) detector. Absorbers used between the source and the detector were of lead, cadmium, and copper.

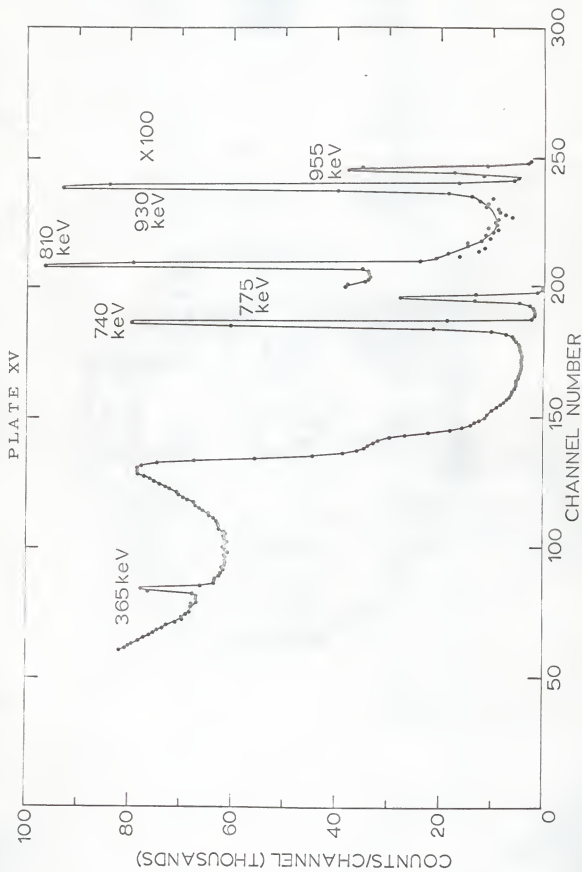


Table 3. Relative intensities of gamma rays from the decay of  $\text{Mo}^{99}$ .

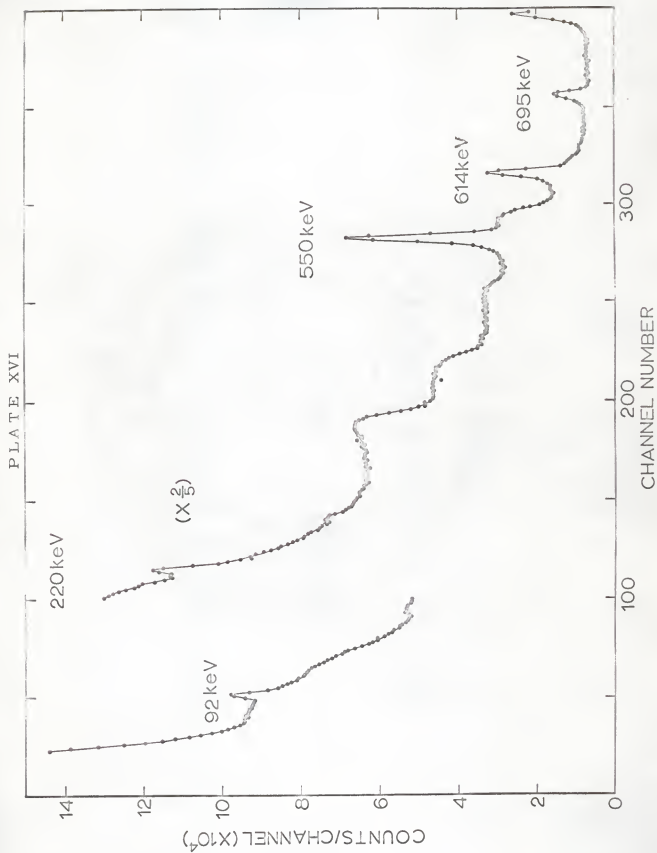
Gamma Ray Energy (keV)	Peak to Total	Efficiency		Relative Intensities				
		Hi E	Lo E	This work	Gretzu & Cappellet & Klingelhofer (2)	Medicus et al. (11)		
140	0.625	---	0.334	2600+200	625	890	900	
181	0.455	---	0.252	160+10	38.8	100	35	
372	0.120	0.0237	0.150	34+2	12.5	11	14	
740	0.035	0.055	---	100	100	100	100	
775	0.0326	0.056	---	32.1+0.7	25	11	---	
810*	0.0298	0.057	---	1.00+0.06	---	---	---	
930*	0.0258	0.058	---	1.16+0.06	---	---	---	
955	0.0250	0.0582	---	0.47+0.04	0.94	---	---	

\* Intensities of 810 keV and 930 keV gamma rays were not known before.

#### EXPLANATION OF PLATE XVI

The low energy gamma ray spectrum of  $\text{Br}^{82}$  accumulated with the RCA 2 mm thick Ge(Li) detector. No absorbers were used between the source and the detector.





#### EXPLANATION OF PLATE XVII

The high energy gamma ray spectrum of  $\text{Br}^{82}$  accumulated with the RCA 2 mm thick Ge(Li) detector. No absorbers were used between the source and the detector.

## PLATE XVII

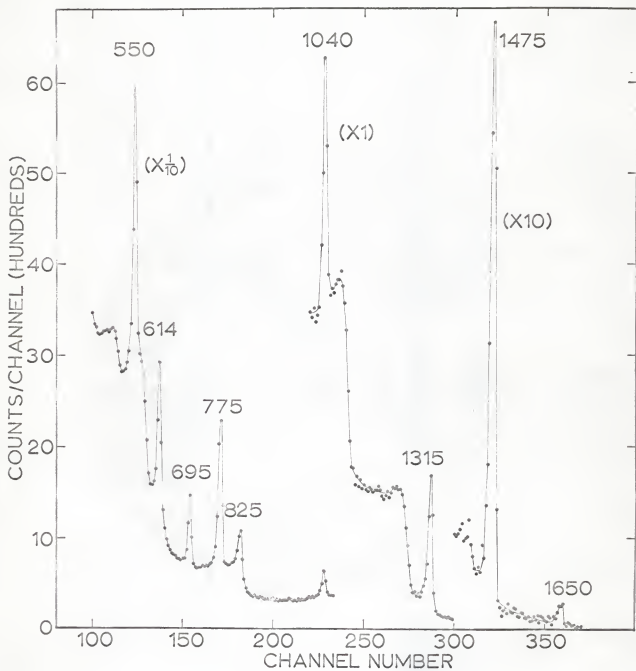


Table 4. Relative intensities of gamma rays from the decay of  $\text{Br}^{82}$ .

Gamma Ray Energy (keV)	Peak to Total	Efficiency	Relative Intensities			
			This work	Hultberg & Hedgran (9)	Benczer-Koller (1)	Waddell & Jensen (15)
92*	0.775	0.310	0.72	---	---	---
220*	0.260	0.116	3.5	---	---	---
550	0.055	0.0683	98.2	80	78	102
614	0.0425	0.065	61	50	50	50
695	0.035	0.062	37	33	34	37
775	0.030	0.059	100	100	100	100
825	0.0275	0.0577	27	30	28	30
1040	0.020	0.054	28	35	35	36
1315	0.0145	0.0467	23.9	32	34	36
1475	0.0125	0.0445	13.0	21	20	18
1650*	0.011	0.0425	0.57	---	---	---

\* The intensities of 92, 220, and 1650 keV gamma rays were not known before.

## APPENDIX

THE EFFICIENCY USED HERE IS THE RATIO OF THE NUMBER OF DETECTED PARTICLES TO THE NUMBER OF PARTICLES ENTERING THE CRYSTAL .

THE TOTAL ATTENUATION COEFFICIENTS ARE IN CM\*\*2/GM.

THE QUANTITY NAN MUST BE AN ODD INTEGER.

UNIT(1) = 1. MEANS THE UNITS ARE IN INCHES.  
 UNIT(1) = 2. MEANS THE UNITS ARE IN MG/CM\*\*2.  
 UNIT(1) = 3. MEANS THE UNITS ARE IN MM.

THE ENERGY IS IN KEV ON THE DATA CARDS.

- 1 REFERS TO THE DETECTOR.
- 2 REFERS TO THE DETECTORS WINDOW.
- 3 REFERS TO THE DETECTORS CASE.
- 4 THROUGH 10 REFER TO THE ABSORBERS.

```

DIMENSION E(60),UM(10,60),THIC(10),DEN(10),NX(10),F1(100),
1F2(100),ELEM(10),UNIT(10),THICK(10)
1 FORMAT(A8,3F8.4/(10F8.4))
2 FORMAT(10F8.5)
3 FORMAT(3(2F8.3,I2))
4 FORMAT( //10X,4HR = ,F5.3,1X,3HIN.,3H = ,F5.3,1X,3HCM.,
110X,4HT = ,F5.3,1X,3HIN.,3H = ,F5.3,1X,3HCM.////)
5 FORMAT(/////19X,4HH = ,F8.5,1X,3HIN., 3H = ,F8.5,4H CM.//
110X,12HENERGY (KEV),7X,
11CHEFFICIENCY, 5X,17HCORRECTION FACTOR//)
6 FORMAT(11X,F10.4,7X,E11.6, 6X,E11.6)
7 FORMAT(24X,6HWINDOW,5X,F7.3,1X,3HIN.,1X,A8)
8 FORMAT(25X,4HCASE,6X,F7.3,1X,3HIN.,1X,A8)
9 FORMAT(I3)
11 FORMAT( 7X,A8,I2,A4,F8.5,10X,A8,I2,A4,F8.5,4X,8HGM/CM**3)
12 FORMAT(1X,F10.4,3X,5(E10.5,3X))

```

```

13 FORMAT(/10X,61H$ORRY, BUT THE ABSORBER STOPS ALL THE PARTICLES WIT
    1H ENERGY ,F8.3,4H KEV/)
14 FORMAT(2X,A6,5H(KEV),3X,5(A3,I2,A1,7X)/)
15 FORMAT(///)
16 FORMAT(1H1,7X,11H1 = CRYSTAL,5X,10H2 = WINDOW,5X,8H3 = CASE,
    15X,16H4-10 = ABSORBERS///)
17 FORMAT(23X,8HABSORBER,4X,F7.3,1X,3HIN.,1X,A8)
18 FORMAT(24X,6HWINDOW,4X,F8.3,1X,8HMG/CM**2,1X,A8)
19 FORMAT(25X,4HCASE,5X,F8.3,1X,8HMG/CM**2,1X,A8)
20 FORMAT(A7,A3,A1,A6,A3)
21 FORMAT(23X,8HABSORBER,1X,F8.3,1X,8HMG/CM**2,1X,A8)
22 FORMAT(I2)
23 FORMAT(1H1,37X,A6/)
124 FORMAT(24X,6HWINDOW,5X,F7.3,1X,3HMM.,1X,A8)
125 FORMAT(25X,4HCASE,6X,F7.3,1X,3HMM.,1X,A8)
126 FORMAT(23X,8HABSORBER,4X,F7.3,1X,3HMM.,1X,A8)
    READ(1,20)DENSIT ,UM1,UM2,ENERGY,EQ
211 READ(1,9)NAN
    IF(NAN.EQ.0)STOP
    READ(1,22)NE
    READ(1,2)(E(I),I=1,NE)
    DO31I=1,10
31 READ(1,1)ELEM(I),THIC(I),UNIT(I),DEN(I),(UM(I,J),J=1,NE)
    READ(1,3)R,DR,NR,T1,DT,NT,H1,DH,NH
    DO42I=1,10
    IF(UNIT(I).EQ.2.)GOTO41
    IF(UNIT(I).EQ.3.)GOTO43
    THICK(I)=THIC(I)*2.54
    GOTO42
41 THICK(I)=THIC(I)/(1000.*DEN(I))
    GOTO42
43 THICK(I)=THIC(I)/10.
42 CONTINUE
    DO34I=1,10
34 NX(I)=I
    WRITE(3,16)
    DO35I=1,9,2
35 WRITE(3,11)DENSIT ,NX(I),EQ,DEN(I),DENSIT ,NX(I+1),EQ,DEN(I+1)
    WRITE(3,15)
    WRITE(3,14)ENERGY,UM1,NX(1),UM2,UM1,NX(2),UM2,UM1,NX(3),UM2,
    UM1,NX(4),UM2,UM1,NX(5),UM2
    DO36I=1,NE
36 WRITE(3,12)E(I),(UM(J,I),J=1,5)
    WRITE(3,15)
    WRITE(3,14)ENERGY,UM1,NX(6),UM2,UM1,NX(7),UM2,UM1,NX(8),UM2
    UM1,NX(9),UM2,UM1,NX(10),UM2
    DO37I=1,NE

```

```

37 WRITE(3,12)E(I),(UM(J,I),J=6,10)
   DO48I=1,10
   DO48J=1,NE
48 UM(I,J)=UM(I,J)*DEN(I)
   R=R-DR
   T1=T1-DT
   H1=H1-DH
   A=ATAN(1.)
   DO10I=1,NR
   R=R+DR
   RR=R/2.54
   T=T1
   DO10J=1,NT
   T=T+DT
   TT=T/2.54
   H=H1
   DO10K=1,NH
   H=H+DH
   HH=H/2.54
   WRITE(3,23)ELEM(I)
   WRITE(3,4)RR,R,TT,T
   DO45I=2,10
   IF(THIC(I).EQ.0.)GOTO45
   IF(UNIT(I).EQ.1.)GOTO46
   IF(UNIT(I).EQ.2.)GOTO47
   IF(UNIT(I).EQ.3.)GOTO120
46 GOTO(90,90,91,91,92,92,92,92,92,92),I
47 GOTO(93,93,94,94,95,95,95,95,95,95),I
120 GOTO(121,121,122,123,123,123,123,123,123,123),I
90 WRITE(3,7)THIC(I),ELEM(I)
   GOTO45
91 WRITE(3,8)THIC(I),ELEM(I)
   GOTO45
92 WRITE(3,17)THIC(I),ELEM(I)
   GOTO45
93 WRITE(3,18)THIC(I),ELEM(I)
   GOTO45
94 WRITE(3,19)THIC(I),ELEM(I)
   GOTO45
95 WRITE(3,21)THIC(I),ELEM(I)
   GOTO45
121 WRITE(3,124)THIC(I),ELEM(I)
   GOTO45
122 WRITE(3,125)THIC(I),ELEM(I)
   GOTO45
123 WRITE(3,126)THIC(I),ELEM(I)
   GOTO45

```

```

45 CONTINUE
  WRITE(3,5)HH,H
  TR=H+T
  IF (TR.EQ.0.)GOTO63
  A=ATAN(R/TR)
  GOTO64
63 A=1.57029635
64 IF (H.EQ.0.)GOTO65
  B=ATAN(R/H)
  GOTO66
65 B=1.57029635
66 CONTINUE
  XY=NAN-1
  DAN=A/XY
  DBN=(B-A)/XY
  DO10L=1,NE
  ARG=0.
  DO61I=2,10
61 ARG=ARG+UM(I,L)*THICK(I)
  IF (ARG.GT.224.)GOTO201
  GOTO210
201 WRITE(3,13)E(L)
  GOTO10
210 ABSORB=1./EXP(ARG)
  AN=-DAN
  BN=A-DBN
  DO4CM=1,NAN
  AN=AN+DAN
  BN=BN+DBN
  XP1=UM(1,L)*T/COS(AN)
  IF (XP1.GT.220.)GOTO50
  F1(M)=(1.-1./EXP(XP1))*SIN(AN)
  GOTO60
50 F1(M)=SIN(AN)
60 IF (H.EQ.0.)GOTO30
  XP2=UM(1,L)*(R/SIN(BN)-H/COS(BN))
  IF (XP2.GT.220.)GOTO70
  F2(M)=(1.-1./EXP(XP2))*SIN(BN)
  GOTO40
70 F2(M)=SIN(BN)
  GOTO40
30 XP3=UM(1,L)*R/SIN(BN)
  IF (XP3.GT.220.)GOTO80
  F2(M)=(1.-1./EXP(XP3))*SIN(BN)
  GOTO40
80 F2(M)=SIN(BN)
40 CONTINUE

```



```
CALL SIMP(NAN,0.,A,F1,VAL1)
CALL SIMP(NAN,A,B,F2,VAL2)
EFF=ABSORB*(VAL1+VAL2)/(1.-COS(B))
CORR=1./EFF
WRITE(3,6)E(L),EFF,CORR
10 CONTINUE
GOTO211
END
```

```
SUBROUTINE SIMP(N,A,B,Y,RESULT)
DIMENSION Y(100)
Y1=0.
Y2=0.
M=N-1
XN=M
H=(B-A)/XN
NEND=M/2
DO 10 I=1,NEND
M1=2*I
Y1=Y1+Y(M1)
M2=2*I-1
10 Y2=Y2+Y(M2)
Y2=Y2-Y(1)
RESULT=H*(Y(1)+4.*Y1+2.*Y2+Y(N))/3.
RETURN
END
```

## ACKNOWLEDGMENT

The author wishes to express his gratitude to Dr. C. E. Mandeville and Dr. V. R. Potnis for their support and guidance during this project. The author also expresses appreciation to Dr. L. D. Ellsworth and E. B. Nieschmidt for help with the electronics and to Dr. P. M. Rinard for writing the first version of the FORTRAN program to calculate efficiencies. This work was supported in part by the National Science Foundation.

## BIBLIOGRAPHY

1. Benczer-Koller, Noémie  
The Beta and Gamma Radiations of  $\text{Br}^{82}$  and  $\text{Rb}^{82}$  and the Energy Levels of  $\text{Kr}^{82}$ . Report, U. S. Atomic Energy Commission, CU-177 (1958).
2. Cappeller, U. and Klingelhöfer, R.  
Über eine  $\gamma$ - $\gamma$ -Winkelkorrelation beim Zerfall von  $^{99}\text{Mo}$  und das Termschema des  $^{99}\text{Tc}$ . Z. Physik 139: 402 (1954).
3. Cretzu, T. and Hohmuth, K.  
Zum Zerfall des  $^{99}\text{Mo}$ . Nuc. Phys. 66: 391 (1965).
4. Dzhelepov, B. and Silant'ev, A.  
Doklady Akad. Nauk SSSR 85: 533 (1952).  
Phys. Abstr. 56, #7890 (1953).
5. Evans, R. D.  
The Atomic Nucleus. McGraw-Hill (1955).
6. Ewan, G. T. and Tavendale, A. J.  
High Resolution Studies of Gamma-Ray Spectra Using Lithium-Drift Germanium Gamma-Ray Spectrometers. Can. J. Phys. 42: 2286 (1964).
7. Fowler, D.  
The Use of Semiconductor Devices in Nuclear Spectroscopy. M. S. Thesis, Kansas State University (1963).
8. Heath, R. L.  
Scintillation Spectroscopy, Gamma-Ray Spectrum Catalogue. U. S. Atomic Energy Commission Report, IDO-16880-1 (1964).
9. Hultberg, Sölve and Hedgran, Arne  
Measurements of the gamma radiations from  $\text{Br}^{82}$  by the method of external conversion. Arkiv Fysik 11: 369 (1957).
10. Johns, H. E., Cormack, D. V., Denesuk, S. A. and Whitmore, G. F.  
Initial Distribution of Compton Electrons. Can. J. Phys. 30: 556 (1952).
11. Medicus, H., Maeder, D. and Schneider, H.  
Der Zerfall des  $^{99}\text{Mo}$  und die Isomerie des  $^{99}\text{Tc}$ . Helv. Phys. Acta 24: 72 (1951).

12. Price, W. J.  
Nuclear Radiation Detection. McGraw-Hill (1964).
13. Storm, E., Gilbert, E. and Israel, H.  
Gamma-ray Absorption Coefficients for Elements 1 through 100 Derived from the Theoretical Values of the National Bureau of Standards. U. S. Atomic Energy Commission Report, LA-2237 (1957).
14. Vegors, S. H. Jr., Marsden, L. L. and Heath, R. L.  
Calculated Efficiencies of Cylindrical Radiation Detectors. U. S. Atomic Energy Commission Report, IDO-16370 (1958).
15. Waddell, R. C. and Jensen, E. N.  
Decay Scheme of  $\text{Br}^{82}$ . Phys. Rev. 102:816 (1956).

THE DETERMINATION OF PHOTON DETECTION EFFICIENCY  
PARAMETERS FOR LITHIUM-DRIFT GERMANIUM DETECTORS

by

Gary Paul Agin

B. S., University of Kansas, 1963

---

AN ABSTRACT OF A MASTER'S THESIS

submitted in partial fulfillment of the

requirements for the degree

MASTER OF SCIENCE

Department of Physics

KANSAS STATE UNIVERSITY

Manhattan, Kansas

1967

The measurement of relative intensities of gamma rays emitted in the decay of a radioactive isotope is useful in studying the properties of the nuclear energy states. In order to obtain relative intensities from an observed spectrum, it is necessary to know the detection properties of the detector. In this work Ge(Li) detectors of two thicknesses, 2 mm and 4.2 mm, were used and detection parameters, full energy peak to total ratio and efficiency, were determined for each.

The full energy peak to total ratio was measured for the 2 mm thick Ge(Li) detector using  $\text{Cr}^{51}$ ,  $\text{Na}^{22}$ ,  $\text{Cs}^{137}$ , and  $\text{Co}^{60}$ . The full energy peak to total ratio was measured for the 4.2 mm thick detector using  $\text{Hg}^{203}$ ,  $\text{Na}^{22}$ ,  $\text{Cs}^{137}$ ,  $\text{Co}^{60}$ , and  $\text{Bi}^{207}$ . The detection efficiency was calculated from tabulated cross-sections for each detector using a computer program written in FORTRAN language.

$\text{Mo}^{99}$  was studied. Gamma rays of energy 140, 181, 372, 740, 775, 810, 930, and 955 keV were found with relative intensities 2600, 160, 34, 100, 32.1, 1.00, 1.16, and 0.47 respectively.

$\text{Br}^{82}$  was also studied. Gamma rays of energy 92, 220, 550, 614, 695, 775, 825, 1040, 1315, 1475, and 1650 keV were found with relative intensities 0.72, 3.5, 98.2, 61, 37, 100, 27, 28, 23.9, 13.0, and 0.57 respectively.

There is reasonably close agreement of the quoted relative intensities with previously published work.